J. Fluid Mech. (1969), *vol.* 35, *part* 4, *pp.* 657–675
Printed in Great Britain

Response of gravity water waves to wind excitation

By JAMES B. BOLE† AND EN YUN HSU
Department of Civil Engineering, Stanford University,
Stanford, California

(Received 7 August 1967 and in revised form 26 September 1968)

The primary objective of this work was to study the response of gravity water waves to wind excitation and, in particular, the applicability of the Miles inviscid shear-flow theory of gravity wave growth, by conducting experiments in a laboratory wind–wave channel under conditions approximating the assumptions of the mathematical model. Mechanically generated wave profiles subjected to wind action were measured with capacitance wire sensors and wave energy was calculated at seven stations spaced at 10 ft. intervals along the channel test section. Waves varied in length from about 2·5 to 6·5 ft. and maximum wind speeds ranged from 12 to 44 ft./sec. Vertical mean air velocity profiles were taken at six stations in the channel, fitted near the air–water interface with semi-logarithmic profiles, and used in a stepwise computation of theoretical wave growth. The results show that the measured wave energy growth is exponential but considerably larger than the growth predictions of Miles's theory. Derived experimental values of the phase-shifted pressure component β are greater than theoretical values by a factor varying from 1 to 10, with a mean of about 3. Wind mean velocity profiles appear to be closely logarithmic near the air–water interface. Wind-generated ripples superposed on mechanically generated waves created a rough water surface with standard deviation larger, in all cases, than the respective critical-layer thickness.

1. Introduction

The mechanism of energy transfer for water wave generation by wind has been an appealing subject of inquiry to fluid dynamicists for many years. The evolution of ideas has culminated in the inviscid shear-flow theory of Miles (1957, 1959), which is mathematically satisfying and convincingly explains the energy transfer to such waves in terms of a hydrodynamic instability. This theory has gained wide acceptance as the explanation of the primary mode of gravity wave growth.

The existing experimental data indicate general support for the theory but are not yet adequate to confirm other than the qualitative applicability of the theory. Quantitatively, most of the experimental results are considerably in excess of Miles's predictions and cannot be interpreted as verifying the theory. Pressure measurements taken in a laboratory wind–wave tank by Shemdin & Hsu (1966) and reported in part in Shemdin & Hsu (1967) show rough agreement with the theory. However, pressure magnitudes and phase shifts are significantly

† Present address: Chevron Oil Field Research Company, La Habra, California.

larger than results given by the theory (based on calculations using measured velocity profiles). Wave growth rates measured in the ocean by Snyder & Cox (1966) and Barnett & Wilkerson (1967) are about eight to ten times larger than theoretical ones (based on the velocity measured at one point above the water surface). Results of other studies, notably those of Inoue (1966), Wiegel & Cross (1966) and Hamada (1963), tend to support indications that the theory underpredicts. Korwin-Kroukovsky (1966) and many other investigators believe flow separation in the lee of waves also to be an important mechanism of energy transfer and attribute discrepancies from Miles's theory to separation effects.

Miles (1967) suggests that the discrepancy between field and laboratory measurements may be explained by an increase with scale [scale factor

$$\Lambda = ky_c(c/U_1)]$$

in the relative importance of wave-induced perturbations in the turbulent Reynolds stresses, which enter into the calculation of the root-mean-square vertical perturbation velocity. He also shows that two mean momentum transfer components, in addition to the component discussed in Miles (1957), may possibly play an important role in wave growth. Because specification of the turbulent Reynolds stresses requires *ad hoc* hypotheses for which there are not adequate experimental data, numerical calculations are not carried out. However, Phillips (1966) concludes that the two components are negligible for conditions under which the critical layer is close to the wave surface.

With the exception of the studies of Shemdin & Hsu and Wiegel & Cross, in which mechanically generated waves were utilized, most of the experimental data have been taken from wave spectra under conditions radically unlike those assumed by the idealized theory, wherein the waves are sinusoidal, two-dimensional and of small amplitude, and the air flow is non-turbulent and hydraulically smooth (a laminar sublayer exists). Inferences about energy transfer mechanisms would therefore seem to be inconclusive. The dearth of wave growth measurements taken under controlled conditions closely comparable to those of Miles's model motivated the present investigation (Bole & Hsu 1967), whose purpose is to examine the applicability of Miles's theory by measuring the growth of mechanically generated waves and studying the growth environment.

2. Wave growth experiments

The wave growth experiments were conducted in a wind–wave channel 6 ft. high, 3 ft. wide and with a usable test section length of 70 ft. (Hsu 1965), under conditions somewhat different from those used by Shemdin & Hsu (1966). A beach for absorbing wave energy and a centrifugal fan for sucking air through the tank were situated downwind of the test section. At the upwind end, the air was drawn vertically through a system of filters and carried horizontally on to the water surface by a converging elbow which was partitioned by three turning vanes. Four-inch thick honeycombs with $\frac{3}{16}$ in. cells were located at the air inlet and exit and served to straighten the flow and decrease the scale of turbulence. A hydraulically driven, horizontal-displacement, wave-generating plate was

17 ft. upstream of the air inlet, a distance sufficient for the generated waves to become fully established before being subjected to wind action. Nominal depths of the water and air media were each 38 in. so that the bottom of the air inlet was 3·5 in. above the water, sufficient clearance for the generated waves of largest amplitude.

Wind–wave combinations selected for the study were governed by considerations of the theory as well as by dynamical features of the experimental facilities. Small-amplitude, deep-water waves with frequencies varying from 0·9 to 1·4 c/s were used with maximum wind speeds varying from 12 to 44 ft./sec (fan speed of 100–300 rev/min). Time records of wave profiles were obtained with capacitance wire sensors at seven locations spaced at 10 ft. intervals along the centreline of the test section; vertical velocity distributions were taken at six intermediate locations with a system comprising a total and a static pressure probe connected differentially across a pressure transducer. Capitance wire output was associated with a Sanborn Series-950 recorder and pressure differential with a Sanborn Series-650 recorder. An Ampex FR-1100 analogue tape recorder was used to record the data.

The velocity profiles were measured without mechanically generated waves, although growing, wind-generated ripples were present. Logarithmic velocity distributions were fitted to the measured data in the boundary-layer region close to the water surface where a logarithmic distribution may reasonably be expected. Measured profiles are indeed closely logarithmic near the water surface.

Wave profile records were analyzed in the following way. A time record of water surface elevation at a given location was phase-averaged over about 35 waves to obtain a mean wave profile. Utilizing the stream function-fitting procedure introduced by Dean (1965) and outlined for application to present conditions by Bole & Hsu (1967), an analytic stream function and the corresponding kinetic and potential energy were determined for each mean wave profile. Total wave energy at each location of the test section was adjusted for wave dissipation found for conditions without wind.

3. Application of the theory

Wave response

Miles's theory assumes a small-amplitude, deep-water, sinusoidal wave with profile shape η expressed as

$$\eta = a\cos k(x-ct) \tag{3.1}$$

or in complex notation as

$$\eta = a\exp[ik(x-ct)] \quad (ka \ll 1), \tag{3.2}$$

where a is the amplitude, k is the wave-number $2\pi/L$, L is the wavelength and c is the wave celerity. The equation of motion governing the propagation of such a wave is

$$\rho_w g\eta + \frac{\rho_w}{k}\frac{\partial^2\eta}{\partial t^2} = -p_a, \tag{3.3}$$

where ρ_w is the mass density of water. The aerodynamic pressure, p_a, acting on the wave has the assumed form

$$p_a = \rho_a U_1^2 ka[\alpha\cos k(x-ct) - \beta\sin k(x-ct)]. \tag{3.4}$$

Thus, p_a is composed of a pressure component proportional to α, in phase with the wave, and a component proportional to β, out of phase with the wave. The terms ρ_a and U_1 are, respectively, the mass density of air and a reference speed for the air, while α and β are dimensionless pressure coefficients that appear as solutions to the aerodynamic boundary-value problem. Equation (3.3) may be solved for the complex wave celerity c:

$$c = c_0\left[1+\frac{1}{2}\frac{\rho_a}{\rho_w}(\alpha+i\beta)\left(\frac{U_1}{c_0}\right)^2\right], \tag{3.5}$$

where

$$c_0 = (g/k)^{\frac{1}{2}}. \tag{3.6}$$

Substituting (3.5) into (3.2) gives an expression for the wave amplitude growth

$$a = a_0 \exp\left[\tfrac{1}{2}kc_0\frac{\rho_a}{\rho_w}\left(\frac{U_1}{c_0}\right)^2\beta t\right], \tag{3.7}$$

where a_0 is the amplitude at $t = 0$. Phillips (1958) has proved that, for a single-component wave in a linearized model, the duration, or time of action t by the wind on the wave, is dynamically equivalent to a fetch or distance x over which the wind has been acting on the propagating wave. This dynamic equivalence, valid for $x \gg L$, is given by

$$x = \tfrac{1}{2}c_0\, t \quad (x \gg L), \tag{3.8}$$

where $\frac{1}{2}c_0$ is the speed of energy propagation or group velocity of a deep-water wave. Introducing (3.8) and (3.6) in (3.7) yields the fetch-dependent amplitude growth

$$a = a_0 \exp\left[\frac{\rho_a}{\rho_w}\frac{k^2}{g}U_1^2\beta x\right], \tag{3.9}$$

where a_0 is now the wave amplitude without wind or at $x = 0$.

The total energy E of a small-amplitude, sinusoidal, progressive, gravity wave is given by

$$E = \tfrac{1}{2}\rho_w g a^2. \tag{3.10}$$

Taking the energy corresponding to a_0 to be E_0, and substituting (3.9) in (3.10) results in the total energy growth

$$E = E_0 \exp\left[\frac{2}{g}\frac{\rho_a}{\rho_w}k^2U_1^2\beta x\right]. \tag{3.11}$$

Wave growth is seen to be exponential and dependent solely on the out-of-phase pressure component β. Wiegel & Cross (1966) arrive at the growth equations (3.9) and (3.11) by integrating the pressure along the wave surface.

Parenthetically, note that the energy growth arising from the pressure distribution assumed by Jeffreys (1925) in his sheltering model is similarly given by

$$E = E_0 \exp\left[\frac{2}{g}\frac{\rho_a}{\rho_w}k^2(U_\infty - c_0)^2\beta_J x\right], \tag{3.12}$$

where β_J is Jeffreys's sheltering coefficient and U_∞ is the wind velocity at the edge of the air boundary layer. This growth equation applies when separation of the air flow exists in the lee of the wave.

Wind excitation

The aerodynamic boundary-value problem is solved for α and β assuming a logarithmic mean velocity distribution in the unperturbed shear flow,

$$U = U_1 \log_e (y/y_0), \tag{3.13}$$

where y_0 is the log intercept, U_1 is the reference velocity defined by

$$U_1 = 2{\cdot}5u_* = 2{\cdot}5(\tau_0/\rho_a)^{\frac{1}{2}} \tag{3.14}$$

and τ_0 is the surface stress exerted tangential to the mean water level. Miles assumes the velocity distribution to be that for turbulent flow over an aerodynamically smooth water surface; that is, smooth enough for an adjacent, so-called laminar sublayer to exist.

Theoretical wave energy (3.11) can be calculated for given wave-numbers using the fitted experimental velocity distributions to obtain U_1 and y_0 and the expression

$$y_c = y_0 \exp (c/U_1) \tag{3.15}$$

to obtain the critical-layer thickness y_c. The critical level is defined as the elevation above the mean water level at which the wave celerity equals the wind velocity. The theory shows β to be directly dependent on the ratio of the second to the first derivative of the mean velocity profile and on the root-mean-square vertical perturbation velocity induced by the wave motion, all evaluated at the critical level. Miles's solution for β (Conte & Miles 1959) is given directly as a function of ky_c.

Wave growth in a developing boundary layer

Because the velocity profiles were taken from within a developing boundary layer, U_1 and β are slowly varying functions of the fetch x. Therefore, in order to accurately evaluate the theoretical wave energy growth along the channel in accordance with the wave measurements taken at 10 ft. intervals, energy must be calculated step by step over each 10 ft. fetch increment using the E of each step as the E_0 of the next. Values of U_1 and β associated with each increment are used to calculate the incremental growth.

The above description may be expressed mathematically in the following way. If $E(i)$, $U_1(i)$, $\beta(i)$ represent parameters associated with the ith 10 ft. fetch increment, the energy ratio increase over the increment is

$$\frac{E(i)}{E(i-1)} = \exp\left[\frac{2}{g}\frac{\rho_a}{\rho_w} k^2 U_1^2(i)\, \beta(i)\, 10\right]. \tag{3.16}$$

The net growth to the Nth i-increment of fetch is

$$\frac{E(N)}{E(0)} = \frac{E(N)}{E(N-1)}\frac{E(N-1)}{E(N-2)} \cdots \frac{E(2)}{E(1)}\frac{E(1)}{E(0)}, \tag{3.17}$$

where $N = x/10$. The latter equation may be expressed as

$$\frac{E(N)}{E(0)} = \exp\left\{\frac{2}{g}\frac{\rho_a}{\rho_w} k^2 (10)\left[U_1^2(1)\,\beta(1) + U_1^2(2)\,\beta(2) + \ldots + U_1^2(N)\,\beta(N)\right]\right\}. \tag{3.18}$$

Taking the logarithm to the base ten of (3.18) leads to

$$\log_{10}\frac{E(N)}{E(0)} = \frac{2\rho_a}{g\rho_w}k^2(10)(\log_{10}e)\sum_{i=1}^{N}U_1^2(i)\beta(i) \tag{3.19}$$

or

$$\log_{10}\{E(F)/E(0)\} = AF, \tag{3.20}$$

where F is a non-dimensional fetch given by

$$F = (10k^2/g)\sum_{i=1}^{N}U_1^2(i)\beta(i) \tag{3.21}$$

and

$$A = (2\rho_a/\rho_w)\log_{10}e. \tag{3.22}$$

For U_1 and β constant with x, (3.21) reduces to

$$F = (k^2/g)U_1\beta x. \tag{3.23}$$

Wave-height growth for small-amplitude waves may be similarly expressed as

$$\log_{10}\{H(F)/H(0)\} = \tfrac{1}{2}AF. \tag{3.24}$$

It is apparent that (3.20) and (3.24) are universal functions prescribing Miles's theoretical wave growth for all combinations of the independent variables. On semilogarithmic graph paper these functions are straight lines with respective slopes of A and $\frac{1}{2}A$. Theoretical wave growth was calculated using (3.20) with F and A given by (3.21) and (3.22). A was evaluated for $\rho_w = 1.00\,\mathrm{g/cm^3}$ and $\rho_a = 0{\cdot}00118\,\mathrm{g/cm^3}$, giving

$$A = 1{\cdot}03\times10^{-3}.$$

4. Results

Velocity profiles

A typical set of velocity profiles taken without mechanically generated waves for a given rev/min setting is exhibited in figure 1. The core flow is seen to accelerate from station to station along the channel, probably due mainly to the flow constriction caused by boundary-layer and wind ripple growth. In all cases the data points near the water appear to follow closely a logarithmic distribution. The lower limit of the measured velocity profile is further from the mean water level with increasing fetch due to the growth of ripples.

The general character of the complete profile is very similar to turbulent boundary-layer profiles measured over solid boundaries. Coles (1956) describes the latter by a wake profile extending toward the boundary from the core flow and a logarithmic profile extending toward the core flow from the boundary, with a smooth transition in the intermediate flow region. The wake profile is a consequence of the constraint provided by inertia, while the logarithmic profile is a consequence of the boundary constraint. In order to obtain the logarithmic, boundary-constrained portion of the velocity profiles such as in figure 1, straight ines were fitted only to those data points close to the boundary.

Figure 2 shows three of the velocity profiles of figure 1 compared with mean profiles taken with mechanically generated waves with respective frequencies and heights of 0·9 c/s, 4 in. and 1·2 c/s, 3 in. It appears that the profiles are nearly the same in the core flow region but in the lower region become slightly offset toward higher velocities while remaining roughly parallel. Mean velocities were

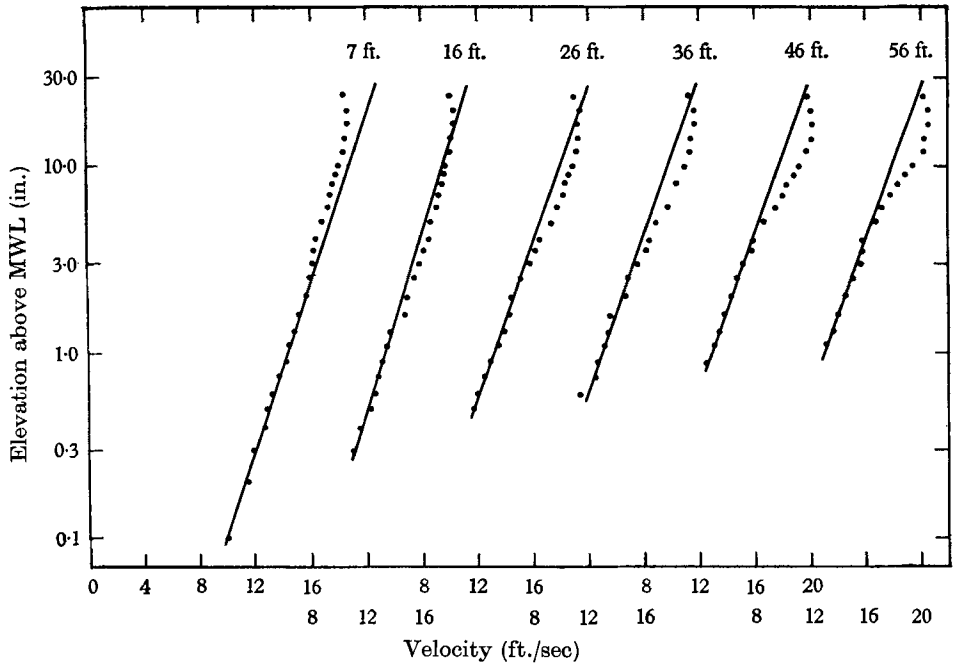

FIGURE 1. 150 rev/min velocity profiles.

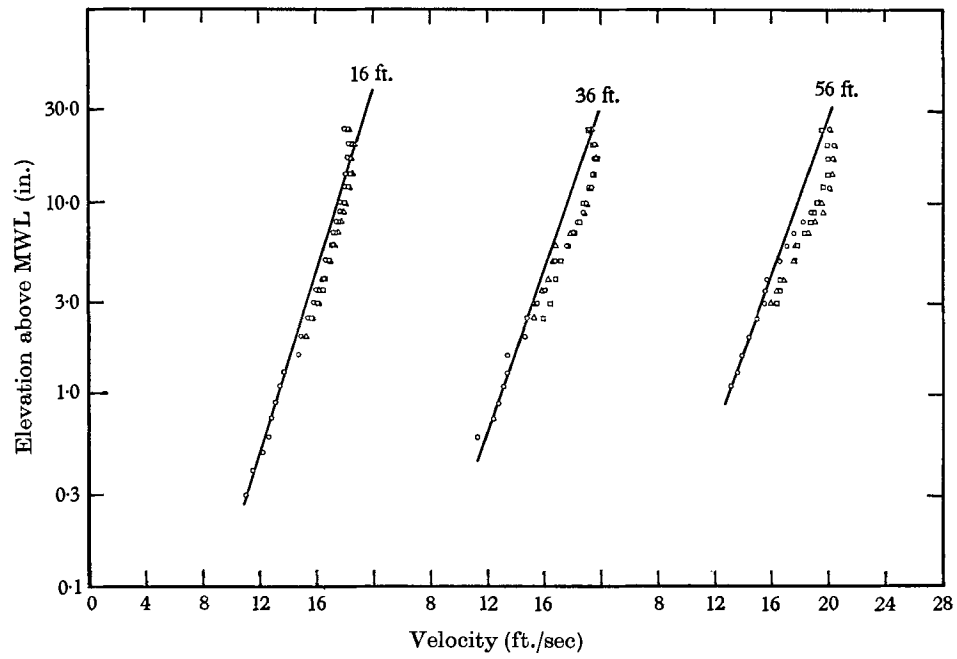

FIGURE 2. 150 rev/min velocity profiles with waves. Mechanical waves: ○, none; □, 0·9 c/s, height = 4 in.; △, 1·2 c/s, height = 3 in.

obtained only down to the wave crests and apparently only a very few points fall in the logarithmic region. As a result of this comparison, it was felt that a much better definition of the logarithmic profile could be obtained by utilizing the profiles taken without mechanically generated waves. This procedure probably gives critical layers slightly too thick and therefore values of Miles's theoretical β slightly too large (say up to 10 %). Values of the parameter U_1 are inversely proportional to the slope of the logarithmic profile and, because the profiles are reasonably parallel, would appear to be little affected by this procedure.

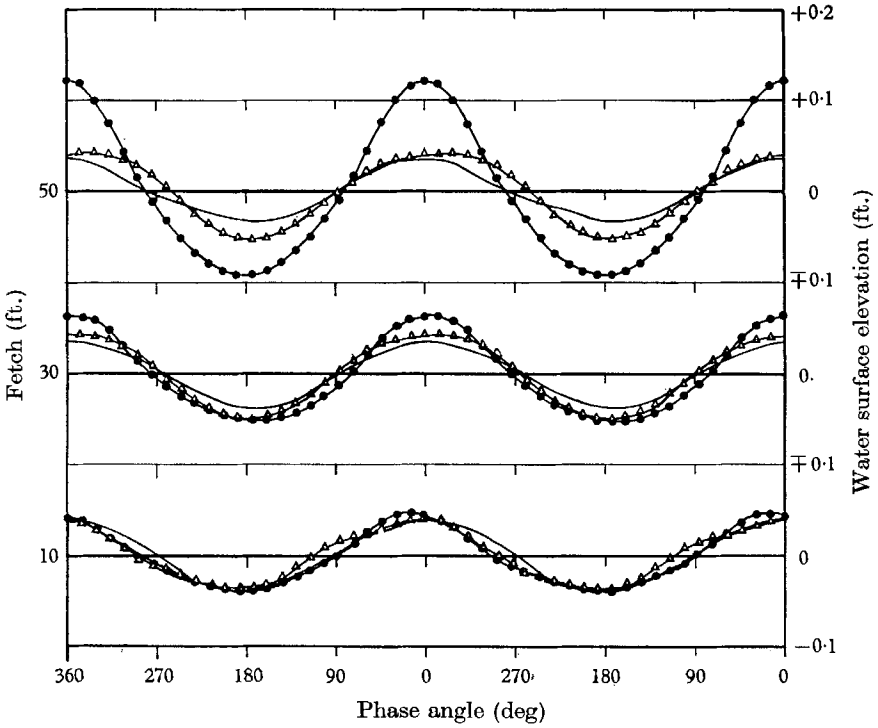

FIGURE 3. 1·3 c/s mean wave profiles. ——, 0 rev/min; △, 200 rev/min; ●, 300 rev/min.

Change in the velocity profiles along the channel at a given fan speed causes fetch dependence in the derived values of β. Increasing boundary stress due to ripple growth and core flow acceleration tends to decrease the slopes of the velocity profiles and to increase velocity magnitudes. Boundary-layer growth tends to do the opposite. The fetch dependence of U_1 and y_0 gives changes in β of 10 to 40 % per wind speed over the range of wind speeds investigated. U_1 values varied from 1·0 to 7·9 ft./sec.

Water surface roughness

The standard deviation about the mean wave profile of a wind-generated ripple spectrum superposed on mechanically generated waves is sharply attenuated compared with the condition without waves. In fact, the attenuation appears to increase as the wave steepness ratio H/L (wave height–length ratio) increases. Ripple standard deviations varied from about 0·001 to 0·039 ft.

and critical-layer thicknesses ranged from about 0·0004 to 0·011 ft. Values of ky_c varied from 4×10^{-4} to 2×10^{-2}, while β varied from 2·0 to 3·45.

In view of the water surface roughness, it seems doubtful that a laminar sublayer could exist or that the organized vortex motion in the critical layer would not be disrupted. Comparison of ripple standard deviations with calculated sublayer and critical-layer thicknesses indicates that the former approximately equals the sublayer and critical-layer thicknesses at a fan speed of 100 rev/min, but at all higher fan speeds is considerably larger than either.

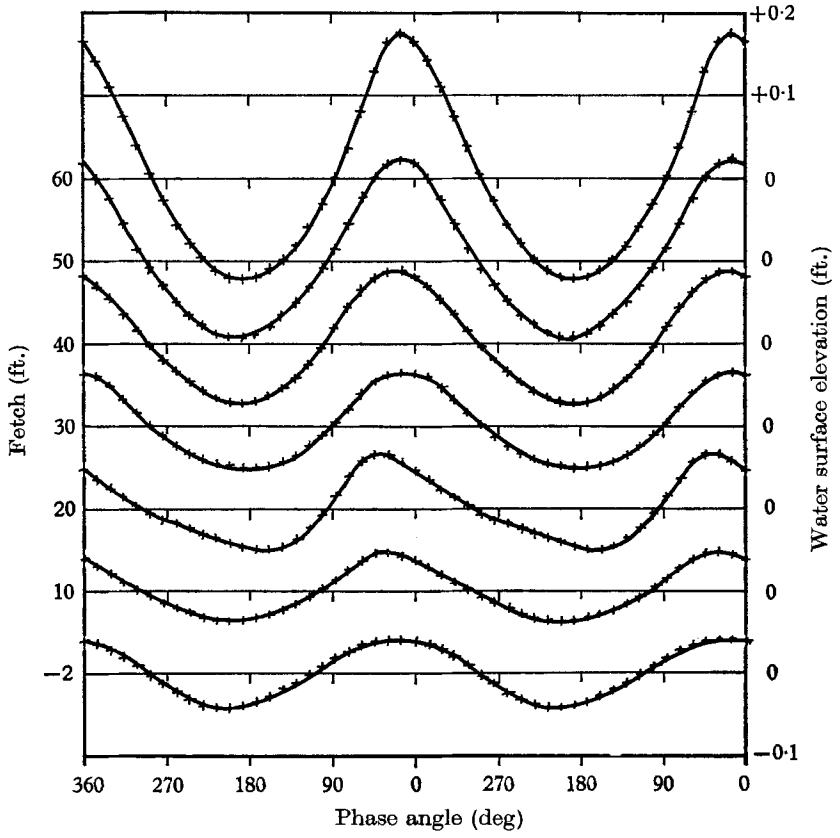

FIGURE 4. 1·3 c/s mean wave profiles at 300 rev/min.

Mean wave profiles

Mean profiles calculated from a series of 35 waves for a 1·3 c/s wave taken at fetches of 10, 30, and 50 ft. and fan speeds of 0, 200, and 300 rev/min are shown superposed in figure 3. The profiles at high frequencies (1·2 to 1·4 c/s) are fairly smooth and symmetrical while those at low frequencies (0·9 to 1·1 c/s) are often irregular, apparently owing to non-random ripple superposition. The original Sanborn recordings reveal that in certain cases the ripples appear to assume certain preferential positions along the wave. Figure 4 displays the growth of a 1·3 c/s wave at seven fetches in the channel for 300 rev/min. Waves are moving toward the left in both of figures 3 and 4.

Wave energy dissipation

The energy calculated for each mean wave profile through the use of the stream-function-fitting procedure was adjusted for experimentally determined viscous dissipation. Dissipation of wave energy was measured at seven stations for conditions without wind. A fitted line gives the mean rate of dissipation, about which there is a random variation of the values at each station. Point departures from the line vary up to 20 %, probably due mostly to the wave reflexion envelope. The net dissipation over the test section ranges up to 25 %; except for two cases that compare favourably, it is about twice as great as that predicted by Hunt (1952) for wall boundary-layer dissipation.

Because there is no way to determine wave energy dissipation when energy is simultaneously being transferred to the waves from the wind, the fitted dissipation curves obtained without wind were used to adjust toward greater values the energy of waves growing under the influence of wind. However, dissipation under the two conditions is not the same. Net energy dissipated increases with total wave energy. Therefore dissipation in the waves growing with wind must be greater than in the waves without wind. In effect, this means that larger values of energy were transferred from the wind to the waves than is indicated by the dissipation-adjusted wave energies.

Wave energy growth

Dissipation-adjusted values of wave energy were normalized on the energy at the second capacitance gauge, located 13 ft. from the air inlet. The normalized values are plotted versus fetch x (referenced to the second capacitance gauge) in figures 5 and 6. Figure 5 shows the dependence of growth on wind velocity for a 1·4 c/s wave and figure 6 shows the dependence on wave frequency at 300 rev/min. There is considerable scatter of data about the best fitted lines but a regular dependency is exhibited. Much of the data scatter is explained by the presence of a reflexion envelope, which can cause random energy variations of up to 20 % due to shifts in its equilibrium position from conditions under which dissipation was measured to conditions under which growth was measured.

For each wave frequency and rev/min, theoretical energy growth was also referenced to the second capacitance gauge by carrying forward the stepwise calculation from this point using the parameters of U_1 and β obtained from the five succeeding downwind velocity profiles. Each of the five stepwise calculations was performed using (3.16); net accumulated growth was found using (3.20), with (3.21) defining the non-dimensional fetch F.

Theoretical and experimental normalized net growth may be plotted at corresponding values of the non-dimensional fetch F. Recall that on a semi-logarithmic plot the ratio of the wave energy at a fetch F to its initial energy can be represented by a single line with a slope of $1{\cdot}03 \times 10^{-3}$. Two such plots are shown in figures 7 and 8. The two plots correspond to those in figures 5 and 6 for respective constant wave frequency of 1·4 c/s and constant rev/min of 300. A scale of H/L on the right of each figure indicates the measured wave steepness. In nearly all cases experimental values fall well above the theoretical line.

The growth curves for most waves are initially fairly linear, indicating exponential wave growth. At larger fetches and especially at higher rev/min, the rate of growth decreases. The variations of growth rate along the fetch exhibit similar behaviour for plots of constant frequency or constant rev/min.

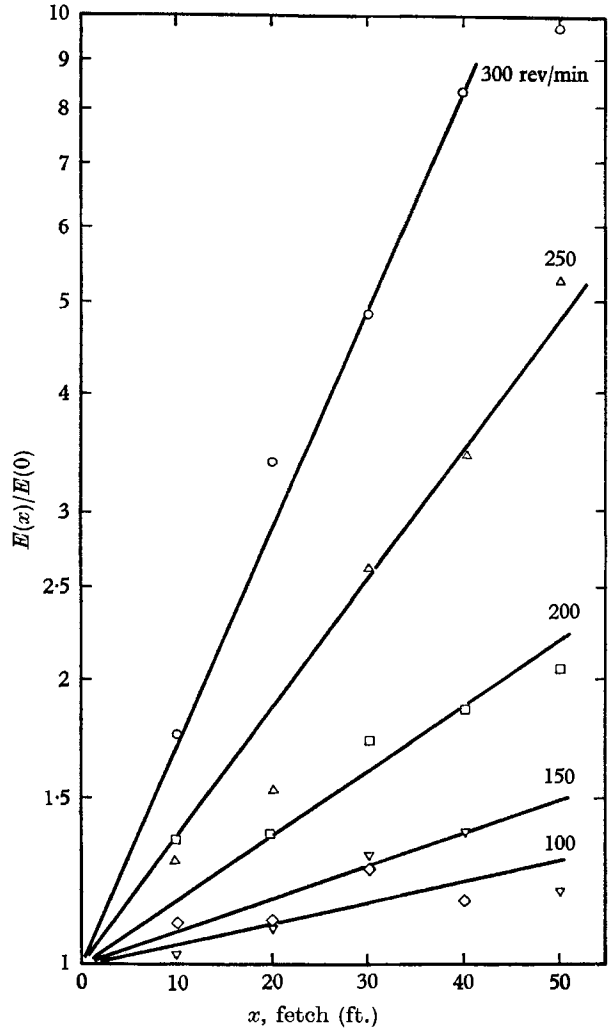

FIGURE 5. 1·4 c/s wave growth *vs.* x.

Comparison of experimental and theoretical β

If one assumes the growth to be totally dependent on F in the form derived from Miles' theory, differences in theoretical and experimental growth must be due to differences in F. Consequently, for each measured growth plotted in figures 7 and 8 it is possible by a simple projection parallel with the F-axis to find the value of F that is given by the intersection with the Miles line. The ratio of the non-dimensional fetch, found by projection for the measured growth (F_M), to the theoretical fetch at which the measured growth is plotted (F_T) is given

directly by the ratio of the respective logarithms of measured and theoretical growth,

$$\frac{F_M}{F_T} = \frac{\log_{10} E_M}{\log_{10} E_T}. \tag{4.1}$$

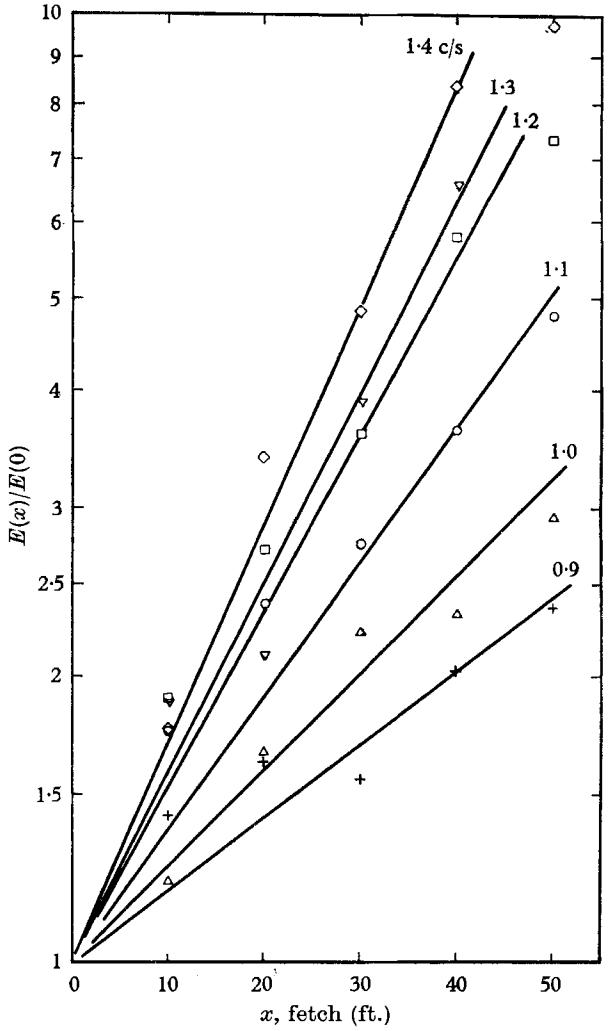

FIGURE 6. Wave growth *vs.* x at 300 rev/min.

This is a ratio of the measured Miles F to the theoretical Miles F for a given wave, fetch and wind velocity profile. Putting (3.21) into (4.1), it can be shown that

$$\frac{(\beta_{\mathrm{av}})_M}{(\beta_{\mathrm{av}})_T} = \frac{\log_{10} E_M}{\log_{10} E_T}. \tag{4.2}$$

Equation (4.2) states that the logarithmic ratio of measured to experimental net growth gives the ratio of average measured β to average theoretical β, where β averages are taken over the step increments to the fetch distance at which net

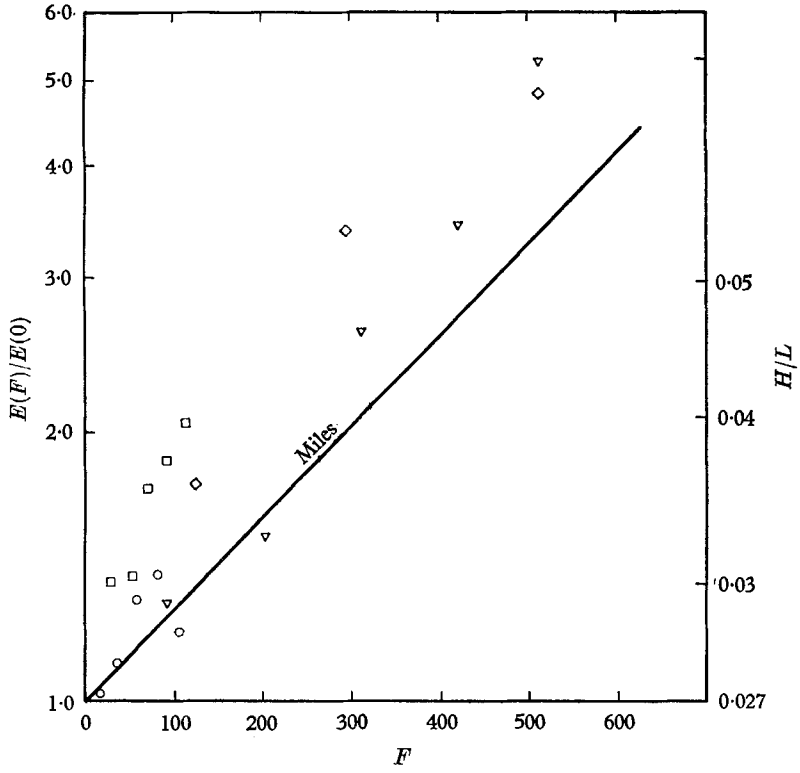

FIGUBE 7. 1·4 c/s wave growth *vs.* F. ○, 150 rev/min; □, 200 rev/min; ▽, 250 rev/min; ◇, 300 rev/min.

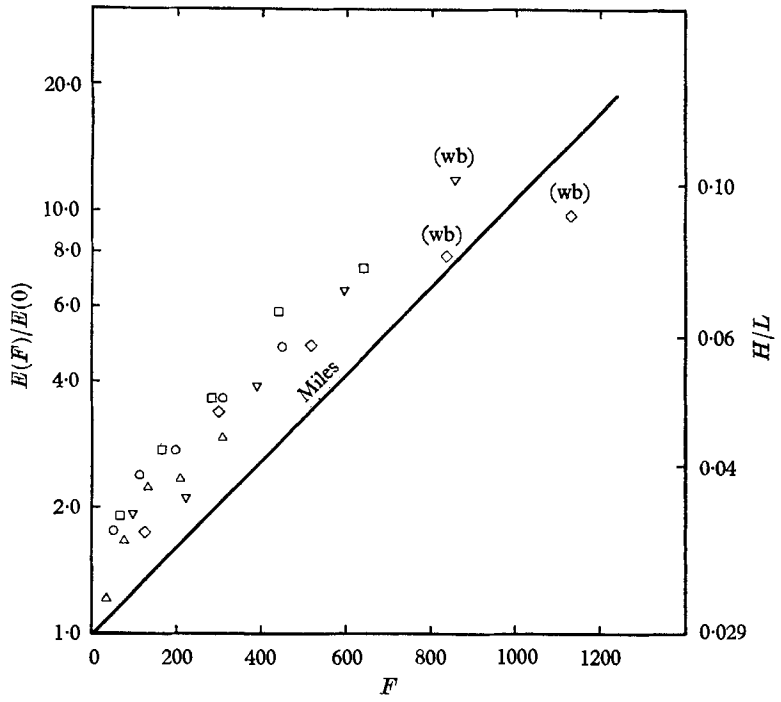

FIGURE 8. Wave growth *vs.* F at 300 rev/min. △, 1·0 c/s; ○, 1·1 c/s; □, 1·2 c/s; ▽, 1·3 c/s; ◇, 1·4 c/s; (wb), wave breaking.

growth is being considered. This ratio has been calculated for all the growth data and is listed in table 1.

The β ratios vary from about 1 to 10. The mean ratio for all frequencies and rev/min is about 3. Values at a wave frequency of 0·9 are consistently above the mean and values at 1·4 are consistently below; at 200 rev/min most values are

Rev/ min	Fetch (ft.)	Mechanical wave frequency (c/s) 0·9	1·0	1·1	1·2	1·3	1·4
100	10	—	—	4·8	4·7	5·4	4·2
	20	—	—	2·2	(−0·4)	11·0	2·4
	30	—	—	1·1	3·1	7·4	3·7
	40	—	—	2·1	2·4	4·4	1·8
	50	—	—	1·8	1·4	6·1	(−0·6)
150	10	7·2	3·1	2·8	1·4	1·5	0·6
	20	2·9	3·2	3·5	1·9	3·8	1·1
	30	1·9	1·3	2·2	3·3	3·7	1·9
	40	3·8	1·3	2·9	2·3	3·9	1·7
	50	3·3	1·3	3·2	2·7	3·5	0·7
200	10	7·2	7·4	9·2	4·0	0·4	4·5
	20	7·3	4·7	7·2	2·2	4·7	2·5
	30	7·7	3·8	7·3	3·6	2·6	3·3
	40	4·8	3·8	5·9	3·5	3·2	2·8
	50	6·1	5·9	5·2	3·6	4·6	2·6
250	10	3·8	2·2	2·9	2·5	1·5	1·1
	20	3·4	2·3	2·4	2·1	1·0	0·9
	30	2·5	2·0	1·9	1·6	0·6	1·3
	40	3·5	1·6	1·9	1·5	1·3	1·2
	50	2·6	1·9	2·0	1·5	1·3	1·4
300	10	7·2	2·7	5·0	4·0	2·8	1·9
	20	4·1	2·9	3·3	2·6	1·4	1·7
	30	2·1	2·6	2·2	1·9	1·5	1·3
	40	2·1	1·7	1·8	1·7	1·3	1·1*
	50	1·8	1·5	1·5	1·3	1·2*	0·9*

* Waves breaking.

TABLE 1. Ratio of experimental to theoretical β (fetch measured from station 13)

well above the mean, while at 250 and 300 rev/min most are well below. There seems to be no clear relation between the values of the β ratio and wave frequency or rev/min.

Shemdin & Hsu (1966) report results of the pressure phase shift θ measured in the same facility at a single small fetch, a condition under which ripple growth is small. These results were converted to values of β (Shemdin 1968) and compared with the theoretical values. The mean ratio of the former to the latter is about 2, in approximate agreement with the present result of 3.

5. Discussion and conclusions

Results of this study indicate that the Miles inviscid shear-flow theory seriously underpredicts wave growth, in general agreement with results reported by several previous investigators. Although experimental conditions were held as nearly as possible to the assumptions of Miles's model, the wave surface was not smooth, causing important differences from the model.

Rough water surface effects

The wind-generated spectrum of ripples superposed on the mechanically generated waves probably interferes with the organized vortex motion in the vicinity of the critical level (Lighthill 1962) in such a way as to modify the physical mechanism of instability. In the case of flow separation in the lee of ripples, this interference could be especially pronounced. If the mean velocity profile at the critical level were even slightly altered by ripple action, the first and second mean velocity derivatives could be changed radically; the perturbation velocities could also be seriously affected. The pressure component β that causes wave growth is directly dependent on these quantities.

The above incompatibilities of the model with natural wave growth conditions were anticipated by Miles. He states in his 1957 paper that 'our model cannot be expected to have more than qualitative significance for rough flow'. The present study supports this expectation. Although the shear-flow theory has not yet been satisfactorily verified for a smooth water surface, it does explain how small-amplitude perturbations excited by wind might grow under special, smooth flow conditions. However, it appears that, once the water surface becomes sufficiently rough, essential elements of the model come into question and the theory can no longer be applied without some modification. Future studies of the natural process of wind wave generation will reveal the extent of the class of cases in which rough flow exists.

Scale factor

The scale factor Λ proposed by Miles varies approximately linearly from 2×10^{-3} to 5×10^{-3} as fetch increases. In the investigation of Shemdin & Hsu (1966), the boundary layer was artificially thickened so that the pressure sensor at the air–water interface could be maintained within the critical layer. Consequently the scale parameters are considerably larger than those of the present investigation and vary from 13×10^{-3} to over 200×10^{-3} at the location where the pressure measurements were made. Comparison of the scale factors for the two investigations indicates that the mean growth parameter β of the present investigation should be smaller than that of the Shemdin study. However, the reverse is true. It thus appears that the scale factor fails to explain the difference in the two mean growth parameters.

Beta factor

The report by Shemdin & Hsu (1966) gives the results of pressure measurements taken within the critical layer over waves ranging in frequency from 0·2 c/s to 0·6 c/s. Several experimental difficulties resulting from instrument limitations

influenced the measurements and data reduction: response characteristics of the wave-following system on which the pressure sensor was mounted caused variation with wave frequency and phase in the distance of the sensor from the wave surface; pressure sensor vibration, caused either aerodynamically or by the discontinuous rotational motion of the electric motor, resulted in random high-frequency fluctuations superimposed on the periodic pressure signals. Average pressure amplitudes were measured for all the waves (0·2, 0·3, 0·4, 0·5, and 0·6 c/s). Comparison of the amplitudes with the theory, reported only for the 0·4 and 0·6 c/s waves, varies from agreement in some cases to a factor of 2 or 3 greater in others. Pressure phase shifts, obtained from the pressure traces using a least-squares fitting procedure, is also reported only for the 0·4 and 0·6 c/s waves. The large spurious pressure fluctuations and the limited sample length of pressure trace each contribute to uncertainty in the calculated phase shifts.

In view of the experimental difficulties, a pressure trace measured under relatively favourable conditions was chosen to be reported in Shemdin & Hsu (1967); these conditions occur for the middle-frequency 0·4 c/s waves. Phase shifts for this wave frequency give values of β that average about 50 % greater than the theoretical values. The values of β for the 0·4, 0·5 and 0·6 c/s waves, reported in Shemdin (1968), have a net average value about twice as great as the theoretical values. Phase shifts for the 0·2 and 0·3 c/s waves have not been reported.

Both the pressure results of Shemdin & Hsu and the present growth results include in β the effects of all mechanisms contributing to a phase shift of the pressure with respect to the wave. The growth results additionally include in β any effects of the rough water surface and of mechanisms that transfer energy through tangential stress. These additional effects may explain some of the difference between the two studies in the mean comparison with theory.

In converting values of phase angle, θ, from the Shemdin & Hsu experimental study to values of β, errors in phase angle become magnified as β errors. Based on the relationship between α and β for small ky_c (Miles 1959), it can be shown that the magnification factor is equal to $2\theta/\tan\theta$ and varies from $-2{\cdot}4$ at a phase angle of 120° to about -10 at 155°. Most of the phase angle data fall within this range. Even though some of the results are in quantitative agreement with the instability theory, the error magnification, along with the difficulties involved in accurately sensing and resolving pressure-wave phase angles, makes quantitative evaluation of the theory inexact.

Energy transfer mechanisms

Two sources of evidence point toward the inapplicability and/or insufficiency of Miles's inviscid theory in predicting the growth of gravity waves under natural sea conditions. The first source is the significantly larger observed rates of wave growth which in the present experiments were measured under conditions simpler than, but similar to, sea conditions. The second is the apparent implication from ripple measurements that assumptions of the theory and physical interpretations of the energy transfer mechanism may no longer hold when the wave surface becomes rough.

This same evidence can be used in support of the argument that separation is perhaps an important additional or substitute mechanism of energy transfer under sea conditions. Separation of the airstream in the lee of waves would cause a greater phase shift than does the instability mechanism and would give a larger sheltering coefficient and growth rate. It was pointed out earlier that either of the coupled mechanisms are associated with exponential growth. These characteristics to be expected from separation are consistent with the measured wave growth.

Ripples riding the waves, even under mild wind conditions, are relatively steep and sharp-crested. Such superposition could easily trigger separation when ripples appear near crests or especially in the lee of waves where the pressure gradient is positive and the tendency to separate already exists. The experimental wave records show many sharp-crested ripple–wave combinations; for some experimental conditions ripple crests riding wave crests appear to be a preferential pattern of superposition.

Non-linear effects

Perhaps the greatest uncertainty associated with the present wave growth measurements is the possibility that significant interaction occurred between the mechanically generated waves and wind-generated ripples. Phillips (1966) argues that non-linear interactions between waves should be weak and the procedure of tracking the response of a single wave-number within a spectrum should be valid. In most of the experimental cases the total spectral energy of the ripples was no more than about 20 % of the mechanically generated wave energy. If wave–wave interaction is indeed weak, the energy transferred to or from the wave should have been a small percentage of its total energy.

A source of slight error arises from the fact that the mean wave profiles are not pure sinusoids, and yet their energy growth is compared with that of Miles's pure sinusoids. An expression made up of a cosine and sine plus their two higher harmonics was least-square fitted to each of the mean wave profiles. Results indicate that at small fetches the mechanically generated waves are closely pure sinusoids, the magnitudes of the sine components and the harmonic cosine components ranging from two to many orders of magnitude smaller than the cosine component. At large fetches the sine term in some cases grew to about one-tenth of the cosine term, giving energy discrepancies of about 1 or 2 % from that of a pure cosine. The total error introduced by the five terms is not greater than 5 % in any case.

Interface flow structure

Interpretation of measured velocity profiles can have a serious effect on how well measurements of wave growth or pressure compare with theory. Because the theory requires knowledge of the mean velocity profile at the critical level and because it was impossible to measure mean velocities at this level, interpretation becomes a problem of how to most meaningfully extrapolate from the measured velocity profile to the critical level. For example, a logarithmic profile fitted to data points further from the water surface would give a larger U_1 and β (for the present data) and therefore a larger theoretical wave growth. Comparison

between measured and theoretical wave growth would then improve. Modification of the mean velocity profiles by the presence of mechanically generated waves could also affect comparison of the experimental results with theory.

Shemdin & Hsu (1966) fitted a logarithmic line to all of the data points in a profile, giving as much weight to velocities in the core flow as to velocities near the boundary. Such a procedure gives critical-layer thicknesses and U_1 values that in most cases are larger than would be obtained by fitting a logarithmic line to only those points near the boundary. For the wave growth they studied, the latter procedure gives larger values of theoretical β and phase shift, and therefore better agreement with measured phase shifts; calculated magnitudes of pressure become smaller owing to the decrease in U_1 and comparison with measured values is poorer.

The uncertainty associated with the flow structure near the air–water interface suggests that experimental investigation of this region is necessary before an understanding of the energy transfer mechanisms and the conditions under which they occur is fully established. Flow separation phenomena associated with wave geometry, ripple superposition and boundary-layer development are complex but could be modelled and fruitfully studied in a wind tunnel as urged by Korwin-Kroukovsky (1966).

This work was supported under a research programme sponsored by the National Science Foundation under Grant GK-736 and the Fluid Dynamics Branch of the Office of Naval Research, U.S. Navy, under contract Nonr 225(71), NR 062-320.

REFERENCES

Barnett, T. P. & Wilkerson, J. C. 1967 On the generation of wind waves as inferred from airborne radar measurements of fetch-limited spectra. *J. Mar. Res.* **25**, 292–328.

Bole, J. B. & Hsu, E. Y. 1967 Response of gravity water waves to wind excitation. *Stanford Univ. Civil Engrg. Dept. Tech. Rep.* no. 79.

Coles, D. 1956 The law of the wake in the turbulent boundary layer. *J. Fluid Mech.* **1**, 191–226.

Conte, S. D. & Miles, J. W. 1959 On the numerical integration of the Orr–Sommerfeld equation. *J. Soc. Indust. Appl. Math.* **7**, 361–6.

Dean, R. G. 1965 Stream function representation of nonlinear ocean waves. *J. Geophys. Res.* **70**, 4561–72.

Hamada, T. 1963 An experimental study of development of wind waves. *Port and Harbour Tech. Res. Inst. Rep.* no. 2, Yokosuka, Japan.

Hsu, E. Y. 1965 A wind, water-wave research facility. *Stanford Univ. Engrg. Dept. Tech. Rep.* no. 57.

Hunt, J. N. 1952 Viscous damping of waves over an inclined bed in a channel of finite width. *Houille Blanche*, **7**, 836.

Inoue, T. 1966 On the growth of the spectrum of a wind generated sea according to a modified Miles–Phillips mechanism. *New York Univ. Dept of Met. and Ocean., Geophys. Sci. Lab. Rep.* no. TR66–6.

Jeffreys, H. 1925 On the formation of water waves by wind. *Proc. Roy. Soc.* A **107**, 189–206.

Korwin-Kroukovsky, B. V. 1966 Air pressures causing wave development, estimate by theory, model tests, and observations. *Dt. hydrogr. Z.* **19**, 145–59.

LIGHTHILL, M. J. 1962 Physical interpretation of the mathematical theory of wave generation by wind. *J. Fluid Mech.* **14**, 385–98.

MILES, J. W. 1957 On the generation of surface waves by shear flows. *J. Fluid Mech.* **3**, 185–204.

MILES, J. W. 1959 On the generation of surface waves by shear flows. *J. Fluid Mech.* **6**, 568–82.

MILES, J. W. 1967 On the generation of surface waves by shear flows. Part 5. *J. Fluid Mech.* **20**, 163–75.

PHILLIPS, O. M. 1958 Wave generation by turbulent wind over a finite fetch. *Proc. 3rd Natn. Congr. Appl. Mech.* pp. 785–9.

PHILLIPS, O. M. 1966 *The Dynamics of the Upper Ocean.* Cambridge University Press.

SHEMDIN, O. H. 1968 Wind generated waves: recent and future developments. *Fifth Space Congress, Oceanography Session, Cocoa Beach, Florida.*

SHEMDIN, O. H. & HSU, E. Y. 1966 The dynamics of wind in the vicinity of progressive water waves. *Stanford Univ. Civil Engrg. Dept. Tech. Rep.* no. 66.

SHEMDIN, O . H. & HSU, E. Y. 1967 Direct measurement of aerodynamic pressure above a simple progressive gravity wave. *J. Fluid Mech.* **30**, 403–16.

SNYDER, R. L. & COX, C. S. 1966 A field study of the wind generation of ocean waves. *J. Mar. Res.* **24**, 141–78.

WIEGEL, R. L. & CROSS, R. H. 1966 Generation of wind waves. *J. WatWays Harb. Div. ASCE* **92**, 1–26.